Comparison between the Laser Beam Ceilometer and an Algorithm for Continuous Evaluation of Cloud Base Height and Temperature, and Cloud Coverage at Local Scale

Esmaiel Malek

Abstract— **The ground-based laser beam ceilometers are used at the Automated Surface Observing Systems (ASOS) in major airports in the U.S. to measure the cloud base height and report the sky conditions on an hourly basis or at shorter intervals. These laser ceilometers are fixed-type whose transmitters and receivers point straight up at the cloud (if any) base. They are unable to detect clouds that are not above the sensor. To report cloudiness at the local scale, many of these types of ceilometers are needed. A single cloud hanging over the sensor will cause overcast readings, whereas, a hole in the clouds above the sensor could cause a clear reading to be reported. To overcome this problem, we have set up a ventilated radiation station at Logan-Cache airport, Utah, U.S.A., since 1995. This airport is equipped with one of the above-mentioned ceilometers.**

This radiation station (composed of pyranometers, pyrgeometers with fields of view of 150º), and net radiometer provide continuous measurements of incoming and outgoing shortwave and longwave radiation and net radiation throughout the year. Considering the additional longwave radiation captured by the facing-up pyrgeometer during cloudy skies, coming from the cloud in the wave band (8-13 µm) which the gaseous emission lacks, we developed an algorithm which provides the continuous cloud information (cloud base height, cloud base temperature, and percent of skies covered by cloud) at local scale during the day and night throughout the year.

Comparisons between the ASOS and the model data during the period June, 2004, are reported in this article. The proposed algorithm is a promising approach for evaluation of the cloud base temperature and height, and percent of skies covered by cloud and its effects on aviation throughout the year.

Keywords- Atmospheric emissivity, atmospheric radiation, ceilometer, cloud parameterization, pyrgeometers.

I. INTRODUCTION

Clouds are visible aggregations of minute droplets of water or tiny crystals of ice suspended in the air. They produce rain or snow, thunder or lightning, rainbows or halos. Clouds play a crucial role in the radiation budget of our planet by the reflecting, absorbing and scattering of solar radiation, and the absorption and re-emission of terrestrial radiation and in the water cycle of the earth-atmosphere system. They also affect the weather and climate by positive or negative feedbacks [1].

In order to understand processes such as global warming and to improve assessment of climate change, it is necessary to improve cloud monitoring systems for distribution of cloudiness at local, regional, and global scales. Therefore, prediction of cloud amount is of great importance to climate modeling. Many researchers have worked on parameterization of clouds to improve their microphysical properties and their effects on the radiation budget and application in general circulation models (CGMs). Unlike other climate variables (e.g., momentum, temperature or moisture), there is no fundamental prognostic equation for cloud fraction [2].

This article addresses application of pyrgeometers, pyranometers and some basic weather parameters to evaluate cloud base height, cloud base temperature, and cloud coverage at local scale throughout the year. Comparisons between cloud data at the Automated Surface Observing Systems (ASOS) and the module output during the period June, 2004, are addressed in this article.

The ground-based laser beam ceilometers at the ASOS in major airports in the U.S. measure the cloud base height and report the sky conditions on an hourly basis or at shorter intervals. These ceilometers are fixed-type and are unable to measure clouds that are not above the sensor [3]. The proposed algorithm is a remedy for this situation.

II. INSTRUMENTATIONS

This research was started in Logan (41º 47' N, 111º 51' W, 1349 m above msl), Utah, U.S.A., in October, 1995. The experimental site is far away from any obstacle, about a quarter of mile from the Automated Surface Observing Systems (ASOS), and is located in the middle of a field covered mostly by cheatgrass (*Bromus tectorum* L.) during the growing season.

Two CM21 Kipp & Zonen pyranometers (one facing down) were used to measure the solar or shortwave radiation.

DOI: 10.5176/2382-5758_2.1.11

The facing-up pyranometer measured the incoming shortwave or solar radiation (R_{si}), and the inverted one measured the outgoing (R_{so}) or reflected shortwave radiation. Two CG1 Kipp & Zonen pyrgeometers (one facing down) were used to measure the longwave radiation. The facing-up measured the incoming longwave (R_{li}) or atmospheric radiation, and the inverted one measured the outgoing longwave (R_{lo}) or terrestrial radiation. Both pyrgeometers and pyranometers have fields of view of about 150^o. The pyranometers and pyrgeometers were equipped with 4 CV2 Kipp & Zonen CVB1 ventilation systems.

An AC power source (110 Volts) was provided to ventilate the Kipp & Zonen radiation system and for heating the rain and snow gage throughout the years. The ventilation air was heated at the rate of 5 W (and occasionally to 10 W) to prevent precipitation of dew and frost, and evaporation of light to moderate rain and snow before reaching the upper pyranometer and pyrgeometer, which otherwise would disturb the measurement, and to suppress the infra-red offset, which is produced by cooling down of the glass domes under calm, clear sky conditions. Figure 1 represents the experimental site along with radiation sensors, the Q 7* net radiometer (Radiation Energy Balance System, Inc., REBS) and other sensors [1]. Figure 2 shows the pyranometers and pyrgeometers. The effects of ventilation on the ventilated pyrgeometer and pyranometer compared to the non-ventilated net radiometer are evident in Figure 3. While the radiometer is covered by frost (in the upper picture) and snow (in the lower picture), the ventilated pyrgeometer and pyranometer are free of these parameters.

The Automated Surface Observing Systems (ASOS) cloud sensor or cloud height indicator (CHI) is a vertically pointed laser transmitter and receiver with a measuring range of 3658 m = 12,000 feet. Its operation is similar to radar in that the time interval between pulse transmission and reflected reception from a cloud base is used to determine the cloud height. The CHI consists of a galliu arsenide laser beam ceilometer operating in the near infra-red (IR) portion of the electromagnetic spectrum at a wavelength of about 0.9 micrometer. The instrument employs light detection and ranging (LIDAR) principles and computer algorithms to provide cloud cover and height information. The frequency range is 620 Hertz (Hz) to 1,120 Hz with a nominal pulse frequency of 770 Hz at room temperature (68 ^{o}F).

Figure 1. The experimental site along with the instruments (see the text for details).

Figure 2- The upper picture shows the facing up pyrgeometer (left) and pyranometer (right). The lower picture shows the same instruments as in the middle picture, but facing down.

The width of the beam is confined to a divergence of ± 2.5 milliradians (mrad) = 0.143^o, so that at 3658 m the beam's sample area is a circle with a diameter of about 2Sin(0.143)* 3658 = 18.26 m = 60 feet. Detail description of the ASOS ceilometer can be found in the National Atmospheric and Oceanic Administration Publications [4].

III. THEORETICAL CONSIDERATIONS

Considering additional longwave radiation captured by the facing-up pyrgeometer during cloudy skies, coming from the cloud in a wave band (8-13 μm) which gaseous emission lacks, we developed an algorithm which provides continuous cloud information (cloud base height, cloud base temperature, and percent of skies covered by cloud) over Cache Valley, Utah, during day and the night throughout the year. The comparisons between the ASOS and the module data during the period of June, 2004, are reported in this article.

Figure 3- The frost-and snow free ventilated pyranometer (upper) and pyrgeometer compared to the non-ventilated net radiometer (lower).

A. Cloudless skies

Many researchers have attempted to formulate the cloudless skies effective atmospheric emissivity ($\varepsilon_{a(cloudless)}$) and atmospheric radiation based on theoretical and empirical concepts. A brief review of some of the past work is reported here. Among them are [5], [6], [7], and [8] who applied either the 2-m actual vapor pressure (e_{a2}), the 2-m air temperature (T_{a2}), or both to compute the cloudless skies emissivity.

The empirical constants *a* and *b* in their equations need to be found. To do that, we selected the 20-min values of measured incoming longwave radiation (R_{lim}) during 12 cloudless days (24-h period) from 1999 through 2003 in Logan (based upon the ASOS and our measurements when the high pressure existed over the region) along with the 2-m moisture and temperature data to find *a* and *b* in the related equation. Reference [9] provides detail information about this analysis.

Despite having almost identical correlation coefficients and Standard Error of Y Estimates (the difference between the measured (R_{lim}) and computed R_{lic}) incoming longwave radiation among the above-mentioned approaches, we chose [7], which have the lowest Std Err of Y Est, for computation of (R_{li}) as:

$$R_{li(Cloudless)} = [0.793 + 4.99 * 10^{-5} * e_{a2} * \exp(1500/T_{a2})] * \sigma * (T_{a2})^4 \quad (1)$$

where e_{a2} is the 2-m actual vapor pressure in mb, T_{a2} is the 2-m air temperature in K, σ is the Stephan-Boltzmann constant = $5.76*10^{-8}$ in W m^{-2} K^{-4} and $R_{li(Cloudless)}$ in W m^{-2}.

B. Cloudy skies

Comparing the incoming atmospheric radiation measured by the pyrgeometer ($R_{li\ (meas)}$) for any sky conditions (cloudless or cloudy) with the one with the one calculated by Idso's formula (Equation 1) for cloudless skies ($R_{li\ (cloudless)}$) yields:

$$A_c = (R_{li(meas.)} - R_{li(cloudless)}) / ((1 - \varepsilon_{a(cloudless)}) * \sigma * T_c^4) \quad (2)$$

where A_c (from zero for cloudless skies to one for overcast skies) and T_c are the cloud amount (percentage) and the cloud base temperature, respectively.

Whenever $R_{li(meas.)}$ is almost equal to $R_{li(cloudless)}$, this implies a cloudless skies. When $R_{li(meas.)} > R_{li(cloudless)}$, the sky conditions could be from partly cloudy to overcast. The hourly comparison of R_{lic} and R_{lim} during the 1999-2003 (1080 observations during days and nights) period is yielded a correlation coefficient R = 0.99.

To solve Equation (2) with two unknowns (A_c and T_c), we used the Poisson's equation, Normand's rule, and the thermodynamic concepts it can be shown that [9] and [10]:

$$\mathrm{Ln}[(T_c + 273.15) / \theta] - 5.01T_c / (240.97 + T_c) + 0.286\mathrm{Ln}(266.5\chi) = 0.0 \quad (3)$$

where θ is the potential temperature in K, and χ is the dimensionless mixing ratio.

After solving Equation (3) for T_c (using a first guess and iterating it by computer until the result comes to zero), the cloud base pressure P_c can be computed as:

$$P_c = 1013.25 \ [(T_c + 273.15) / \theta]^{3.496} \quad (4)$$

The cloud base height H_c and thus the cloud type (i.e., low, middle or high clouds) can be evaluated as:

$$H_c = 100T_{a2} \ [1 - (P_c / P_{a2})^{0.293}] \quad (5)$$

where P_{a2} is the air pressure at 2 m. Also, Equation 2 can be used to determine the percent of sky covered by clouds. To expand the network at regional scale, the satellite link (i.e., the NOAA GOES West satellite) will allow constant monitoring of the radiation systems' performance and maintenance scheduling on an "as needed" basis [11].

IV. RESULTS AND DISCUSSIONS

As shown, having the parameters required in Equation (1), the cloudless atmospheric radiation can be estimated quite reasonably. The period of 8-12 June, 2004, at the Logan airport was chosen to compare the model and ASOS ceilometer outputs. Cloudless and cloudy skies along with precipitation events are included in this period. These two sites are less than a mile apart from each other. The 20-min values of 2-m relative humidity (RH_2) and air temperature (T_{a2}), surface temperature (T_{sur}), and precipitation in Logan during the period of 8-12 June, 2004, are depicted in Figure 4. The total precipitation amounted to 21.7 mm during this period. Also, the afternoon temperature lags (T_{sur} - T_{a2}) are evident in this figure.

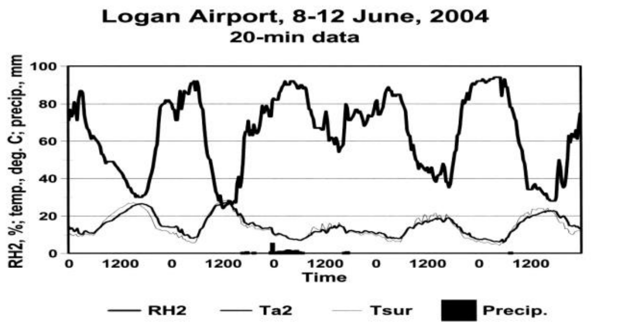

Figure 4- The 20-min values of 2-m relative humidity (RH_2) and air temperature (T_{a2}); surface temperature (T_{sur}); and precipitation in Logan during the period of 8-12 June, 2004.

Figure 5 presents the 20-min amounts of radiation components, namely: incoming (R_{si}) and outgoing (R_{so}) solar (shortwave); and the incoming atmospheric (R_{li}) and outgoing terrestrial (R_{lo}) longwave; and net (R_n) radiation in Logan during the period of 8-12 June, 2004.

As shown in Figure 5b, the closeness of R_{li} and R_{lo} is a good indication of cloudiness and possible precipitation (day or night). These clouds could be formed overhead or developed over the surrounding areas in this valley. Those overhead are captured both by the ceilometer and the instruments at the radiation station. The surrounding clouds can be viewed only by the radiation instruments. As a result, many hours of cloudiness not reported by ASOS were captured by the model. This is because of the 150^o field of the instruments used in the module. Ceilometer views the sky only vertically.

The measured (R_{lim}) and computed (R_{lic}) incoming longwave radiation, percent of sky covered by clouds, the cloud base height during 8-12 June, 2004, are depicted in Figure 6. As shown in Figure 6a, whenever R_{lim} is almost identical to R_{lic}, cloudless sky can be expected. The bigger the difference between R_{lim} and R_{lic} in Figure 6a yields up to almost overcast sky and possible precipitation.

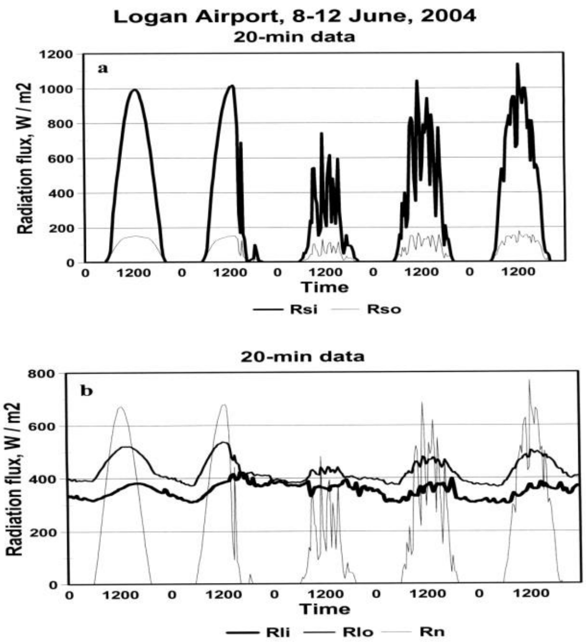

Figure 5 a) The 20-min amounts of radiation components, namely: incoming (R_{si}) and outgoing (R_{so}) solar (shortwave), and b) the 20-min values of incoming atmospheric (R_{li}) and outgoing terrestrial (R_{lo}) longwave, and net (R_n) radiation in Logan during the period of 8-12 June, 2004.

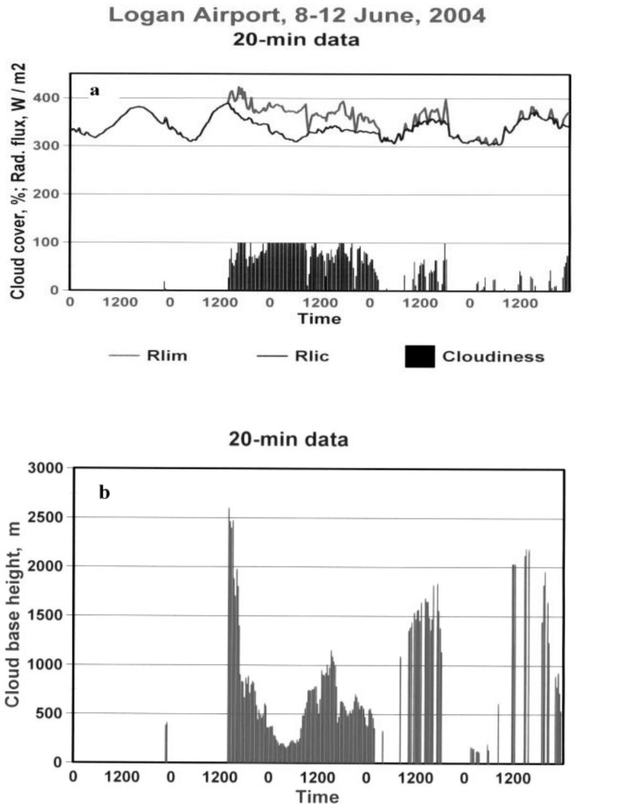

Figure 6 a) The measured (R_{lim}) and computed (R_{lic}) incoming longwave radiation, percent of sky covered by clouds, and b) the cloud base height during 8-12 June, 2004.

The cloud amounts below 3658 m reported by ASOS are in five categories: clear (CLR, means when the cloud coverage is from zero up to 5 %), few (FEW, from 5 up to 25 % coverage), scattered (SCT, from 25 up to 50 % coverage), broken (BRK, from 50 up to 87 % coverage), and overcast (OVC, from 87 up 100 % coverage). ASOS computer algorithms also round the cloud base height to the nearest 30.48 m (100 feet) for: clouds between the surface and 1524 m (5000 feet), to the nearest 152 m (500 feet) between 1524 m and 3048 m (10,000 feet) and to the nearest 305 m (1000 feet) for height above 3048 m. Our model does not provide cloud layers, instead the overall cloud coverage and cloud base height are denoted by numbers at local scale during each 20 minutes or shorter periods.

Figure 7a presents the percent of hourly cloudiness evaluated by the model and reported by ASOS in Logan during the period of 8-12 June, 2004. As shown, there were many hours of cloudiness not reported by ASOS during this period, but depicted by the instruments. Also shown, there are periods when ASOS reported almost occasional overcast skies for a cluster of single clouds above the ceilometer, for instance, in the morning of 11 June, 2004; but considering the field of view of the instruments used in the model, this cloud covers only a small fraction of the sky. The cloud base heights reported by ASOS and the model are revealed in Figure 7b. As shown, the heights computed by the ASOS algorithms are mostly greater than those evaluated by the model. The difference can be related to the different layers distinguished by ASOS.

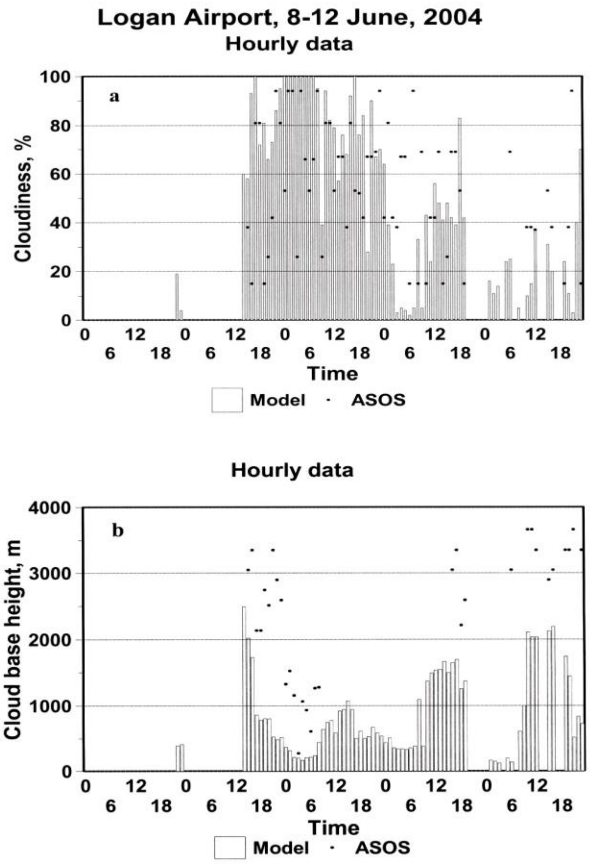

Figure 7 a) The percent of hourly cloudiness evaluated by the model and reported by ASOS (NOAA, 2004) and b) the cloud base heights reported by ASOS and the model are revealed in Logan during the period of 8-12 June, 2004.

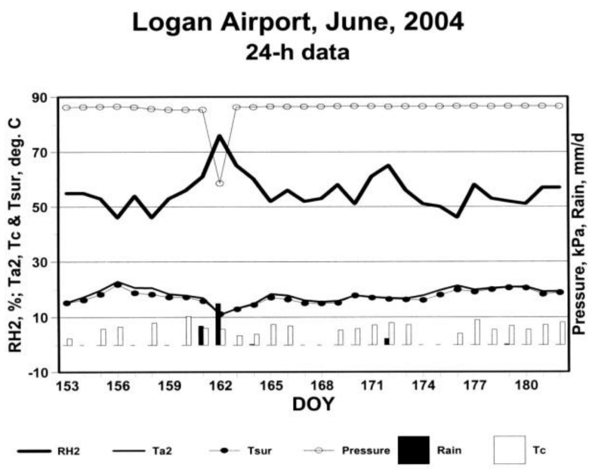

Figure 8- The 24-h mean surface pressure, surface temperature, 2-m air temperature and humidity, cloud base temperature during June 2004 at the experimental site.

The 24-h mean surface pressure, surface temperature, 2-m air temperature and humidity, cloud base temperature are depicted in Figure 8. The occasional precipitation in Figure 8 during this summer-time dry spell is the result of development of thermal low and cumulonimbus activity (a convective phenomenon).

Figure 9 presents the 24-h values of the radiation budget components in Logan during June, 2004. The average albedo = 100 (R_{so} / R_{si}) was about 18 percent, with minor increases during rainy events in this month.

Figure 10 depicts the difference between the measured and calculated incoming atmospheric radiation and cloudiness during June, 2004, in Logan. Equal values of the measured and calculated incoming atmospheric means cloudless skies. Cloudiness could have happened during portions of days and nights, or occasionally an entire 24-h period during this month.

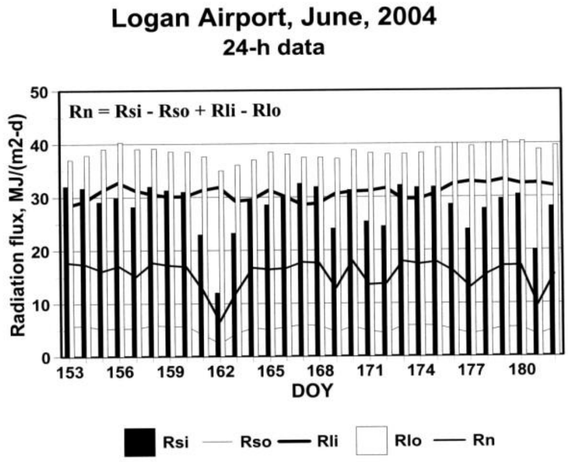

Figure 9. The 24-h values of the radiation budget components in Logan during June, 2004.

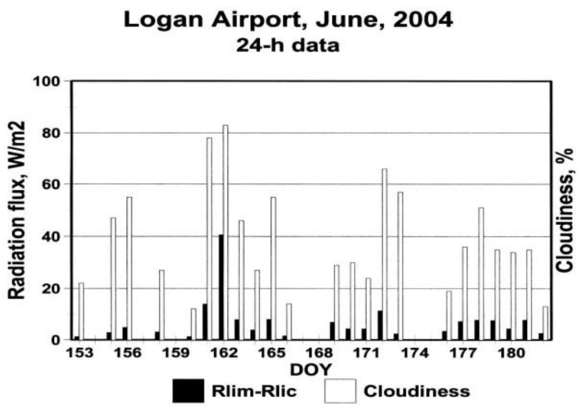

Figure 10- The difference between the measured and calculated incoming atmospheric radiation and cloudiness during June, 2004, in Logan, Utah.

Figure 10 depicts the difference between the measured and calculated incoming atmospheric radiation and cloudiness during June, 2004, in Logan. Equal values of the measured and calculated incoming atmospheric are indications of cloudless skies. Cloudiness could have happened during portions days and nights, or occasionally an entire 24-h period during this month.

V. CONCLUDING REMARKS

The U.S. National Oceanic and Atmospheric Administration (NOAA) issues infra-red (IR) and visible (VS) images of clouds over the western U.S. and most of the Pacific Ocean via its Geostationary Observational Environmental Satellite (GOES) three times during a 24-h period. Comparison was made between the IR, and VS cloud images at 5:30 a.m., 11:30 a.m., and 5:00 p.m. local time, respectively, and the model output during 8-12 June, 2004. Images showed a cloudless sky over Cache Valley during 8 June through around noon on 9 June, 2004. The model also shows the same sky conditions during this period. Both images and model show cloudiness starting on early afternoon of 9 June throughout 10 June, 2004. Both model and images indicate cloudless and cloudy skies during the morning and afternoon, respectively, of 11 June, 2004.

There was also good agreement on cloudiness conditions between the model and images on 12 June, 2004. As shown, the proposed algorithm is a promising approach for evaluation of cloud base temperature and height, and more importantly, the percent of skies covered by cloud at the local scale. The differences between cloud cover and cloud base height between the model and ASOS are attributed to the ASOS algorithms. While a ceilometer is not able to see clouds outside the diameter of 18.26 m at 3658 m vertically above, the model depicts these clouds over surrounding areas. Having enough pyrgeometers and the necessary surface weather parameters, the study can be expanded to regional scale for continuous evaluation of clouds (if any).

As shown, the proposed algorithm is a promising approach for evaluation of cloud base temperature and height, and more importantly, the percent of skies covered by cloud at the local scale. The differences between cloud cover and cloud base height between the model and ASOS are attributed to the ASOS algorithms.

ACKNOWLEDGMENT

This research was supported by Utah State University, the Utah Agricultural Experiment Station, and Embry-Riddle Aeronautical University. The author wishes to express his thanks to all.

REFERENCES

[1] E. Malek, "Evaluation of cloud feedback at local scale: warming or cooling?" J. Environ. Sci. and Eng. N. 3B, Vol. 4, 2015. doi:10.17265/2162-5263/2015.04.006.

[2] K.E. Trenberth (Ed). "Climate System Modeling". Cambridge Univ. Press. 1992, 788 pp.

[3] C.D. Ahrens and R. Henson, "Meteorology today: An Introduction to Weather, Climate, and the Environment (11th Ed.)". Cengage Learning, 2016, 586 pp.

[4] National Oceanic and Atmospheric Administration (NOAA). Automated Surface Observing System (ASOS), 1998. User's Guide, 82 pp.

[5] D. Brunt. Notes on radiation from the atmosphere. Quart. J. Roy. Meteorol. Soc. 1992, 58: 389 - 418.

[6] W.H. Brutsaert. "On a derivable formula for longwave radiation from clear skies". Water Resour. Res., 1975, 11: 742- 744.

[7] S.B. Idso. "A set of equations for full spectrum and 8-14 μm and 10.5-12.5 μm thermal radiation from cloudless skies". Water Resour. Res. 1981, 17: 295-304.

[8] J.L. Monteith, and M.H. Unsworth. "Principles of Environmental Physics". Edward Arnold, New York. 1990, 291pp.

[9] E. Malek, "cloud contribution to the daily and annual radiation budget in a mountainous valley". 2008, Atmos. Res.367-380.

[10] E. Malek. "Evaluation of effective atmospheric emissivity and parameterization of cloud at local scale". 1997, Atmos. Res. 45:41-54.

[11] E.Malek, G.E. Bingham, and G.D. McCurdy. "Evapotranspiration from the margin and moist playa of a closed west desert valley. 1990, J. Hydrol. 120: 15-34.

AUTHOR'S PROFILE

Dr. Esmaiel Malek earned PhD in Biometeorology, which relates life and weather. He has taught numerous courses of meteorology and climatology at under graduate and graduate levels at Utah State and at Embry-Riddle Aeronautical Universities since 1985. He has published on evaluation of energy and water balance components, harnessing of solar and wind energies, evapotranspiration, water and air pollution, and cloud modeling at local scale. Additionally, he served as the Interim Director and Associate Director of the Climate Center at Utah State University. He is a member of the American Meteorological Society and a Certified Consulting Meteorologist (CCM).